LIGHTWEIGHT COMPOSITE COMPONENTS FOR A RALLY COMPETITION CAR

Gabriel Fortin[1], Akio Ohtani[1], Hiroyuki Hamada[2], Kanta Ito[3], Takanori Kitamura[3]

[1] The Department of Advanced-Fibro Science, Kyoto Institute of Technology, Matsugasaki, Sakyo-ku, Kyoto, 606-8585, Japan

[2] The Future-Applied Conventional Technology Centre, Kyoto Institute of Technology, Matsugasaki, Sakyo-ku, Kyoto, 606-8585, Japan

[3]Daiwa Itagami Co., Ltd., 5-32 Kawahara-cho, Kashiwara-shi, Osaka, 582-0004, Japan

Keywords: Sandwich Panels, Cardboard, Carbon fiber, Compression, Bending

ABSTRACT

This project focuses on the integration of polymer matrix composite materials in structural components of a professional rally competition car. More specifically, the parts involve sandwich composite panels consisting of lightweight corrugated cardboard cores and carbon fibre cloth skins manufactured using a wet lay-up process. There is growing interest in incorporating cardboard materials in composite parts due to its vast availability, low density, low cost, and use of recycled paper sources. Variations to the sandwich composite core and skins are applied and their effects on the final mechanical properties are investigated. The performance of the cardboard cores is assessed in the parts by varying the cardboard thickness and the specific type of cardboard flute liner paper. Two cardboard thicknesses (AF type = 3 mm and KF type = 5 mm) and two cardboard flute liner areal densities (C5 = 160 g/m^2 and K5 = 170 g/m^2) are compared. The effects of the number of carbon fiber fabric sheets on the sandwich skins is also studied. Panels with one and two plies of carbon fabric face sheets are compared. The quality of the manufactured parts is measured qualitatively by visual observation, and quantitatively by performing compression and bending tests. The average through-thickness compressive strength, bending strength, and bending rigidity of the parts is presented. The experimental results are compared with the mechanical properties obtained from sandwich panel theoretical predictions. Visual observations of the sandwich panel cross sections reveal a resin-rich region within the panels on the side in contact with the bottom tool during wet lay-up. A modified manufacturing process involving rotating the panels throughout consolidation and cure is later introduced to uniformly redistribute the resin through-thickness to ensure optimal and balanced mechanical properties.

1 INTRODUCTION

Sandwich composite structures are an excellent choice for applications demanding very high stiffness and lightweight requirements [1]. The typical structure of a sandwich panel that consists of stiff skins separated by a low-density core ensures that optimal stiffness and low-weight characteristics can be obtained. The mechanical properties of sandwich structures made of corrugated cardboard cores and woven carbon fiber cloth skins for potential use in vehicle crash and impact protection regions have not been thoroughly investigated. As corrugated cardboard offers a cost-effective and lightweight solution for sandwich structure cores, its mechanical performance under compression and bending loading conditions needs to be studied. As part of an initiative to manufacture composite structures for vehicle weight reduction and suitable crash protection, sandwich panels with varying cardboard core and carbon fiber skin thicknesses are manufactured using a hand lay-up process and are evaluated by mechanical testing.

2 EXPERIMENTAL METHODS

2.1 Material Specifications

The performance of the sandwich panels is assessed in the parts by varying the cardboard thickness and the specific type of cardboard liner paper. A typical cardboard structure is shown in figure 1.

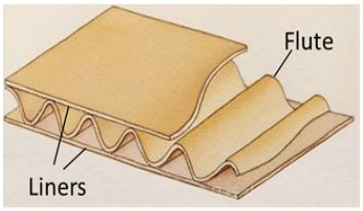

Figure 1: Sketch of the cardboard structure.

Two cardboard thicknesses (AF type = 3 mm and KF type = 5 mm) and two cardboard liner areal densities (C5 = 160 g/m^2 and K5 = 170 g/m^2) are compared. The areal density of the carboard flute is kept constant at 120 g/m^2. The two cardboard types are illustrated in figure 2. Panels with zero, one and two plies of plain-weave carbon fabric face sheets are manufactured using a hand lay-up process and the effects of the number of carbon fabric sheets on the sandwich skins is studied.

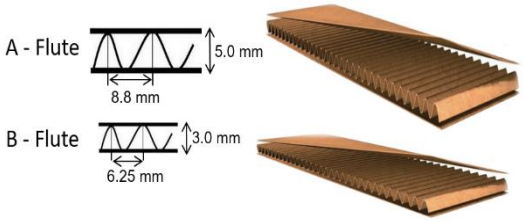

Figure 2: A and B cardboard flute types.

2.2 Hand Lay-up Manufacturing Process

The hand lay-up process of manufacturing cardboard-carbon fiber sandwich panels involves stacking the materials from bottom to top as illustrated in the sketch of figure 3. The dimensions of the cardboard panel and carbon fiber cloth are 300 mm × 300 mm.

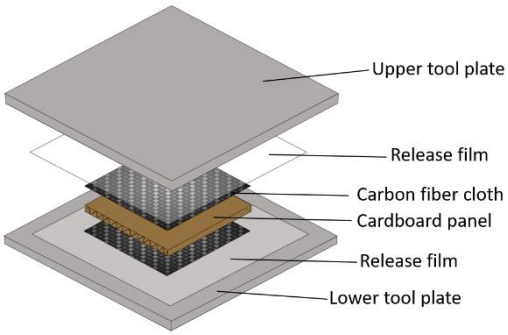

Figure 3: Tooling and materials required for hand lay-up.

The following steps were followed in chronological order: (1) applying and evenly spreading 40 mL of vinylester resin on the top surface of a release film on a flat tool using a roller; (2) applying one or two layers of carbon fiber cloth sheets as required on top of the resin and allowing the resin to impregnate the carbon cloth for 2 minutes; (3) evenly spreading the resin within the carbon cloth using a roller over the entire surface; (4) applying another 40 mL of resin over the carbon cloth and spreading it over the entire surface with a roller; (5) applying 40 mL of resin on one side of the cardboard and allowing the resin to soak into the paper for 1 minute; (6) gently placing the wet face of the cardboard directly onto the wet carbon cloth from the previous step and applying firm hand pressure to steady the cardboard in place; (7) applying 40 mL of resin on the other cardboard face and allowing a soak time of 1 minute; (8) placing one or two carbon fibre cloths onto the wet cardboard face and allowing the

resin to impregnate the fibres for 2 minutes; (9) evenly spreading the resin within the carbon cloth using a roller over the entire surface; (10) applying 40 mL of resin over the carbon cloth and spreading it over the entire surface with a roller; (11) applying 50 mL of resin over the centre of the carbon cloth without any spreading; (12) applying a release film on the top surface; (13) and lastly, resting a flat steel plate and weights to allow a consolidation pressure of 0.6 MPa at room temperature for 24 hours. The part is then removed from the tooling and fully cured in an oven at 100°C for 2 hours.

2.3 Sample Preparation and Mechanical Testing

From each panel, three specimens each for compression and three-point bending tests were cut. The dimensions of the compression samples are 40 mm × 40 mm, and the dimensions of the bending samples are 140 mm long by 40 mm wide. Example compression and bending samples from a cardboard and cardboard-carbon sandwich panel are shown in figure 4. The bending samples were cute such that the flute length direction lies parallel to the length and span of the sample during bending.

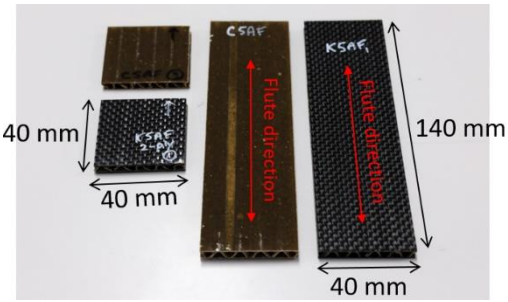

Figure 4: Dimensions of samples for compression and bending tests.

Once the specimens were cut, thickness measurements with a digital micrometer were taken at 5 locations on the compression samples, and at 3 locations on the bending samples near the likely region of failure at mid-span. The exact width of the bending specimens in this region was also measured 3 times with digital calipers.

The compression and bending tests were performed in an instron machine with a 10 kN load cell at a crosshead speed of For the compression tests, the A-flute samples testing speed was set at 1.0 mm/min and the B-flute sample testing speed was set to 0.6 mm/min to account for the difference in carboard thicknesses. The compression load-displacement curves were obtained for all samples.

Three-point bending tests were performed on all samples at a speed of 1.0 mm/min. The span of the samples between the bottom two supports was fixed at L = 100 mm. The bending load-displacement curves were obtained for all samples. Prior to mechanical testing, visual observations of the sample cross-section and overall shape were also noted.

3 RESULTS AND DISCUSSION

3.1 Compression Testing

The compression load-displacement curves for all samples were recorded and the maximum failure stress was obtained by dividing the applied load by the area of the sample (40 mm × 40 mm). An example of the stress-strain curves for the sandwich panels with 2 carbon plies on the skin is presented in figure 5. Due to the large number of samples in this study, the stress-strain curves for the cardboard only and cardboard with 1 carbon ply on the skin have not been included in this paper. The maximum failure stress for all the samples are summarized in figure 6 and table 1. The error bars in figure 6 represent the maximum and minimum values of the 3 samples tested for each dataset.

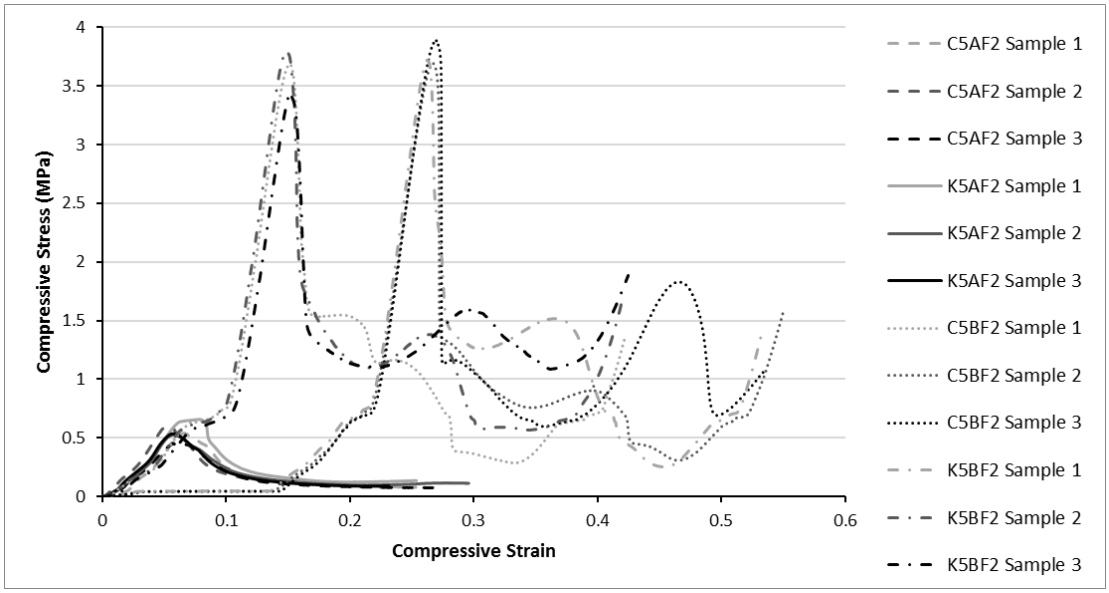

Figure 5: Compressive stress-strain curves of a cardboard sandwich panel with 2 carbon plies on the skins.

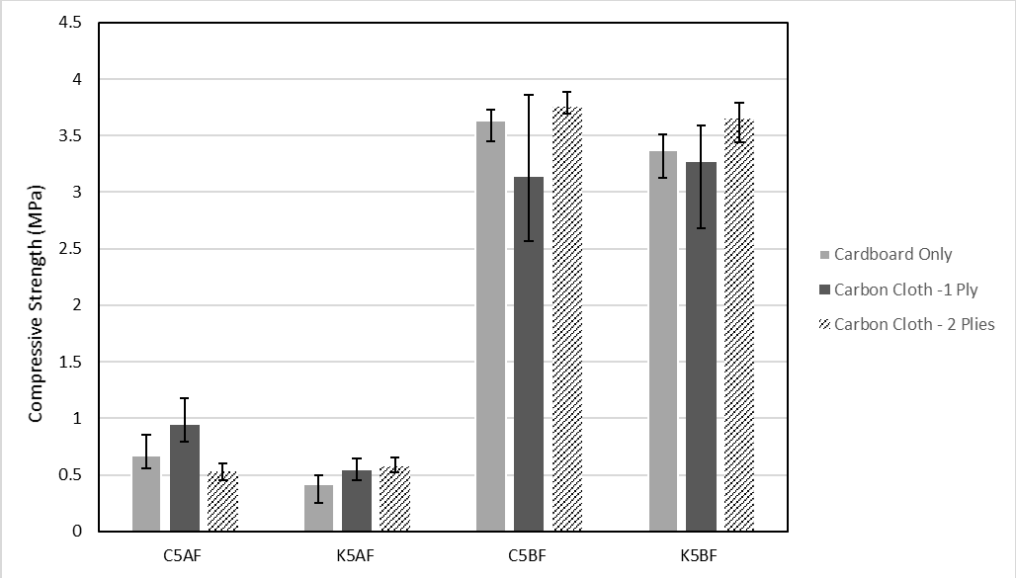

Figure 6: Summary of the compressive strength for all tested samples.

Table 1: Summary of the average compressive strength for all tested samples.

Cardboard Type	Average Compressive Strength (MPa)		
	Cardboard Only	1 carbon ply skin	2 carbon ply skins
C5AF	0.67	0.94	0.53
K5AF	0.42	0.54	0.57
C5BF	3.63	3.13	3.76
K5BF	3.37	3.26	3.65

From the compression testing results, it is evident that the strength of the B-flute samples (thinner than the A-flute samples) is significantly greater. There is no significant difference in strength between

the C5 and K5 cardboard liner types, and there is no noticeable difference between samples with 0, 1, or 2 plies of woven carbon skins. The compressive strength is clearly dominated in this case by the cardboard structure and thickness (A-flute vs. B-flute).

3.2 Bending Tests

An example of the load-deflection curves obtained from the 3-point bending tests is shown in figure 7, for the sandwich samples with 2 woven carbon plies. The maximum stress for the samples was computed from the load data by combining and rearranging the equations for the 2nd moment of area of a rectangular beam (equation 1), and the maximum bending stress (equation 2) in the form of equation 3.

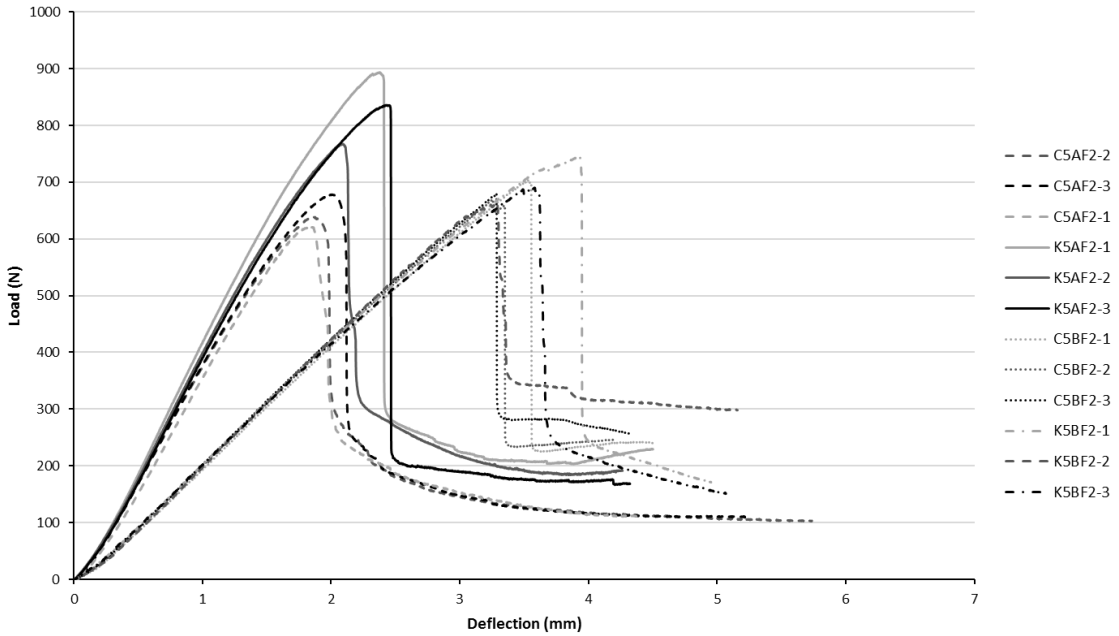

Figure 7: Load-deflection curves for bending specimens with 2 carbon plies on the skins.

$$I = \frac{bh^3}{12} \tag{1}$$

$$\sigma = \frac{Mc}{I} \tag{2}$$

$$\sigma = \frac{3FL}{2bh^2} \tag{3}$$

Where *b* is the width of the sample, *h* is the height of the sample, *M* is the bending moment, *F* is the applied load on the sample, and *L* is the span of the sample (100 mm). The averages of the bending strength with the maximum and minimum range for each panel type are presented in figure 8.

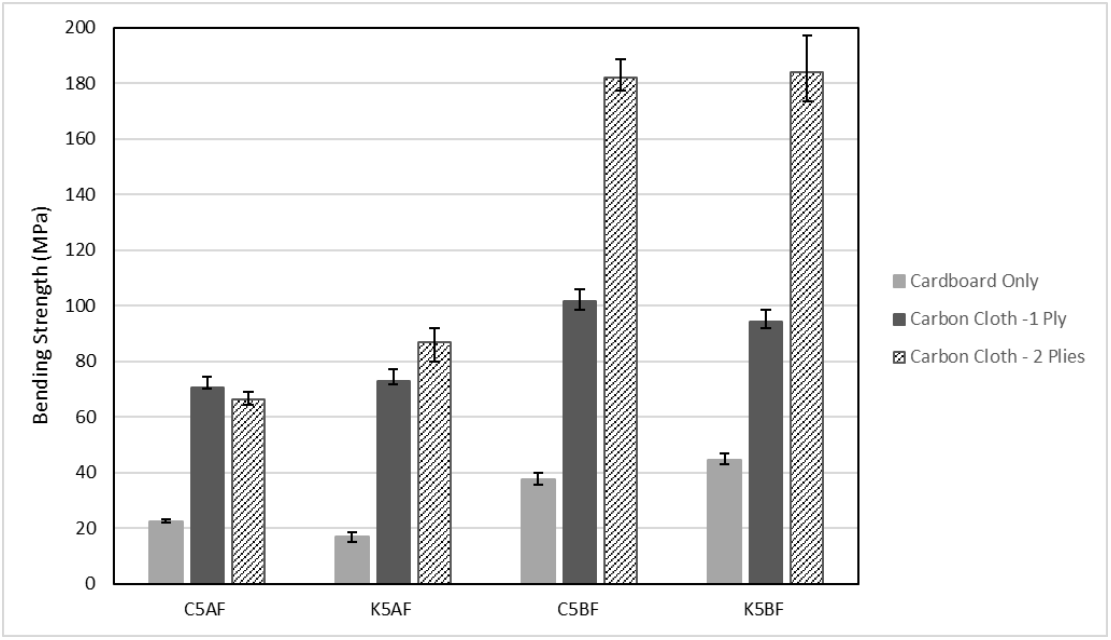

Figure 8: Summary of the bending strength for all tested samples.

From the results, the B-flute samples are strongest in bending, especially with two carbon plies on the skins. The B-flute samples are significantly stronger with 2 carbon plies as opposed to 1 or no carbon plies. For the A-flute cardboard samples, there is no significant difference in strength between samples with 1 or 2 carbon plies. However, the A-flute samples with carbon plies are considerably stronger than the A-flute samples with no carbon plies at all. Overall, there is also no notable difference between the C5 and K5 liner paper type.

The flexural modulus of the samples was calculated from the load-deflection curves using equation 4 [2]:

$$E = \frac{L^3}{4bh^3} \times \frac{\Delta F}{\Delta s} \tag{4}$$

Where *b*, *h*, and *L* are as defined in equation 3, and $\frac{\Delta F}{\Delta s}$ is the slope of the linear portion of the load-deflection curve. A summary of the average flexural modulus for all tested samples and the range of values is presented in figure 9.

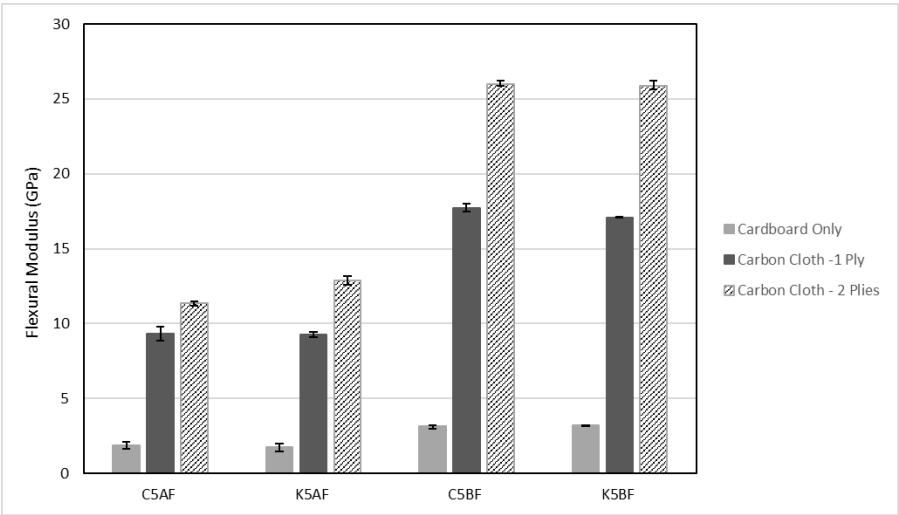

Figure 9: Summary of the average flexural modulus values for all samples.

Similar conclusions to the bending strength values can be made with the flexural modulus. The flexural modulus is not greatly affected by the liner paper type (C5 vs K5) and depends primarily on the flute structure (A vs B type). The modulus of the B-flute samples is significantly greater, especially with the C5BF and K5BF samples that have 2 carbon plies. The effect of additional carbon plies is not as significant for the C5AF and K5AF samples.

3.3 Resin-rich region

During cutting of the samples prior to mechanical testing, a resin-rich region was observed in all samples, with and without carbon plies. An example resin-rich side of a panel is shown in figure 10.

Figure 10: Resin-rich region shown at the bottom of the sample.

The resin accumulates inside the cardboard liner face, on the bottom edge. Careful examination of the orientation of the samples during hand lay-up reveals that the resin-rich side corresponds to the surface of the panel in contact with the bottom tool, as sketched in figure 11.

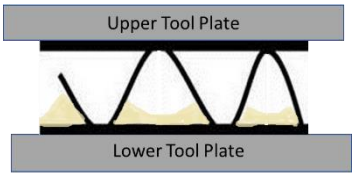

Figure 11: Resin-rich region inside the surface in contact with the lower tool plate during hand lay-up.

Due to the asymmetry from the resin-rich region, bending tests were repeated for all samples with the resin-rich side facing downwards. In section 3.2, all bending tests were performed with the resin-rich side facing up. A comparison of the flexural strength and modulus values is presented in tables 2 and 3, respectively.

Table 2: Comparison of the flexural strength values with the resin-rich side facing up and down.

Sample	Average Flexural Strength (MPa)					
	Resin-rich side up			Resin-rich side down		
	Number of carbon plies			Number of carbon plies		
	0	1	2	0	1	2
C5AF	22.51	70.31	66.24	18.98	38.33	45.74
K5AF	16.82	72.79	86.87	18.08	34.89	69.02
C5BF	37.31	101.72	181.91	48.13	103.87	167.88
K5BF	44.43	94.12	183.93	47.39	89.00	156.83

Table 3: Comparison of the flexural modulus values with the resin-rich side facing up and down.

Sample	Average Flexural Modulus (GPa)					
	Resin-rich side up			Resin-rich side down		
	Number of carbon plies			Number of carbon plies		
	0	1	2	0	1	2
C5AF	1.87	9.34	11.36	2.11	9.15	11.63
K5AF	1.72	9.24	12.90	2.04	9.20	12.89
C5BF	3.13	17.72	25.99	3.64	18.85	26.63
K5BF	3.19	17.10	25.86	3.53	18.09	25.96

When comparing the flexural strength values, there is no significant difference between the samples with 0 carbon plies. For samples with 1 ply of carbon fiber, the strength decreases significantly in the C5AF and K5AF samples when the resin-rich side is facing down. For samples with 2 plies of carbon fiber, a decrease in the flexural strength occurs in all the samples. Visual observation of the failure surface of all samples with carbon fiber skins reveals that crushing of the core on the top surface occurs (compressive side of the sample). When the resin-rich layer is on the top surface, it contributes to greater strength of the compressive side. When the resin-rich side is on the bottom, the samples still fail by compression of the core on the top surface, with no additional strength from excess resin.

3.4 Warpage

The asymmetry of the panels due to the resin-rich region also likely contributes to the warpage observed in every part upon removal from the tool. An example of the warpage present in a bending sample is shown in figure 12.

Figure 12: Warpage observed after removal from the tool.

All parts warped in the same direction relative to the upper and lower tool plates, as sketched in figure 13.

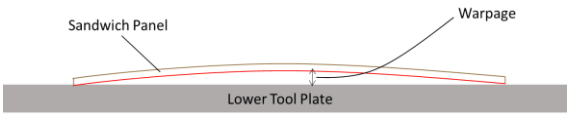

Figure 13: Warpage direction relative to the tool surface.

The red line corresponds to the resin-rich side of the panel. All parts, with and without carbon fiber skins, warped away from the lower tool. The additional shrinkage of the lower surface of the panel due to excess resin curing is likely the cause of the warpage. As the resin-rich region contracts during cure, compressive stresses are locked in the bottom surface.

3.5 Theoretical predictions of flexural rigidity

The flexural rigidity of a sandwich panel can be predicted with the following equation [1]:

$$D = \frac{E_{fx} b t^3}{6} + \frac{E_{fx} b t d^2}{2} + \frac{E_{cx} b c^3}{12} \quad (5)$$

Where E_{fx} is the Young's modulus of the face sheet or skin, b is the width of the sample as previously defined, t is the thickness of the skin, d is the distance that separates the mid-point of the top and bottom skins, E_{cx} is the modulus of the core material, and c is the thickness of the core. In most cases for thin skins, the middle term of equation 5 accounts for almost all the rigidity, and equation 5 can therefore be simplified as follows [1]:

$$D = \frac{E_{fx} b t d^2}{2} \quad (6)$$

The geometric variables in equation 6 are represented in figure 14. The thickness of each ply on the skin is measured as approximately 0.22 mm.

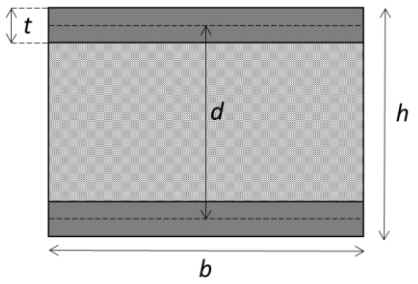

Figure 14: Sandwich panel geometric variables for calculating rigidity.

The sandwich panel skins in this project consist of plain-weave carbon fabric sheets. The exact modulus of the woven material after wet lay-up is not currently known, however for simplification, can be approximated to 0/90 unidirectional plies. Using a carbon fiber longitudinal modulus of 230 GPa [3], vinylester modulus of 3.6 GPa [4] and a fiber volume fraction of 50%, classical laminate theory software predicts a modulus of approximately 60 GPa for this material. Incorporating the modulus of the skins and the geometric variables in equation 6, the predicted flexural rigidity values are obtained and presented in table 4.

The experimental theoretical rigidity can simply be obtained by multiplying the obtained flexural modulus from section 3.2 with the second moment of area of a rectangular structure as in equations 7 and 8:

$$D = EI \tag{7}$$

$$D = \frac{E_{exp} b h^3}{12} \tag{8}$$

The results of the experimental values for flexural rigidity are also compared in table 4.

Table 4: Experimental and predicted flexural rigidity.

Sample	Flexural Rigidity (MN-mm^2)	
	Experimental	Predicted
C5AF1	5.48	7.94
K5AF1	5.12	7.56
C5BF1	2.19	2.64
K5BF1	2.21	2.72
C5AF2	8.32	17.03
K5AF2	9.22	16.71
C5BF2	4.58	5.94
K5BF2	4.63	6.02

The predictions are in the same order of magnitude, but consistently high compared to the experimental values. The predictions for C5AF2 and K5AF2 especially are significantly high. Further work needs to be conducted to verify the material properties of the woven carbon skins in this analysis.

4 CONCLUSIONS

In this study, the bending and compression properties of composite sandwich panels made from cardboard cores and woven carbon fiber skins using a hand lay-up process were investigated. The main findings of this project are as follows:

- The compressive strength is greatest for the B-flute samples which are thinner than the A-flute samples. There is also no observable difference between the compressive strength of C5 and K5 liner types.
- The bending strength is greatest for the B-flute samples, especially for the B-flute samples with 2

carbon fiber plies on the skin. A similar trend applies for the measured flexural modulus.

- A resin-rich region is present inside the surface of the panel in contact with the lower tool during hand lay-up. As a result, warpage is present on all samples upon removal from the tool.
- Bending tests performed on samples with the resin-rich side up and the resin-rich side down reveal the effect of resin distribution on the bending properties. In certain cases, the resin plays an important role in providing strength on the upper side of the sample.
- Predictions of flexural rigidity based on sandwich panel theory over predict the values based on the experimental measurements. The material properties and assumptions used in the analysis should be further analyzed.

The following recommendations for future work are proposed:

- Modifying the hand lay-up process such that the resin rich-region is avoided. This would involve rotating the panel and tooling upside-down throughout consolidation at specified time intervals. Trials should be performed on small samples with small tooling such that the part and tool can easily be handled at first.
- Integration of a cardboard sandwich composite structure in an application for vehicle crash energy absorption.

ACKNOWLEDGMENTS

The authors would like to acknowledge Daiwa Itagami, Co., Ltd. for supplying all of the cardboard materials that were tested in this study.

REFERENCES

[1] Petras, A. (1998). Design of Sandwich Structures (Ph.D). University of Cambridge.

[2] ASTM. (2015). Standard Test Methods for Flexural Properties of Unreinforced and Reinforced Plastics and Electrical Insulating Materials (ASTM D790). West Conshohocken, PA, USA: ASTM International.

[3] Mounier, D., Poilane, C., Bucher, C., & Picart, P. (2012). Evaluation of transverse elastic properties of fibers used in composite materials by laser resonant ultrasound spectroscopy. Societe Francaise d'Acoustique. Acoustics 2012, Nantes, France.

[4] Rocha, V., Fernandez, R., & Duran, O. (n.d.). The mechanical properties of glass fiber reinforcement in vinyl ester resin. Academia, 2017.